

## Chiral dynamics of $\Sigma$ hyperons in the nuclear medium

N. Kaiser

Physik-Department T39, Technische Universität München, D-85747 Garching, Germany

(Received 3 February 2005; published 6 June 2005)

Using SU(3) chiral perturbation theory, we calculate the density-dependent complex mean field  $U_{\Sigma}(k_f) + iW_{\Sigma}(k_f)$  of a  $\Sigma$  hyperon in isospin-symmetric nuclear matter. The leading long-range  $\Sigma N$  interaction arises from one-kaon exchange and from two-pion exchange with a  $\Sigma$  or a  $\Lambda$  hyperon in the intermediate state. We find from the  $\Sigma N \rightarrow \Lambda N$  conversion process at nuclear matter saturation density  $\rho_0 = 0.16 \text{ fm}^{-3}$  an imaginary single-particle potential of  $W_{\Sigma}(k_{f0}) = -21.5 \text{ MeV}$ , in fair agreement with existing empirical determinations. The genuine long-range contributions from iterated (second order) one-pion exchange with an intermediate  $\Sigma$  or  $\Lambda$  hyperon sum to a moderately repulsive real single-particle potential of  $U_{\Sigma}(k_{f0}) = 59 \text{ MeV}$ . Recently measured ( $\pi^-$ ,  $K^+$ ) inclusive spectra related to  $\Sigma^-$  formation in heavy nuclei give evidence for a  $\Sigma$ -nucleus repulsion of similar size. Our results suggest that the net effect of the short-range  $\Sigma N$  interaction on the  $\Sigma$  nuclear mean field could be small.

DOI: 10.1103/PhysRevC.71.068201

PACS number(s): 13.75.Ev, 21.65.+f, 21.80.+a, 24.10.Cn

The  $\Sigma$ -nucleus optical potential describes the behavior of a  $\Sigma$  hyperon in the nuclear medium. The quantitative determination of this (complex) potential is a subject of current interest. Whereas an earlier analysis of the shifts and widths of x-ray transitions in  $\Sigma^-$  atoms came up with an attractive (real)  $\Sigma$ -nucleus potential of about  $-27 \text{ MeV}$  [1] (i.e., almost equal to the well established attractive  $\Lambda$ -nucleus potential of depth  $-28 \text{ MeV}$  [2]), there is currently good experimental and phenomenological evidence for a substantial  $\Sigma$ -nucleus repulsion. A reanalysis of the  $\Sigma^-$ -atom data by Batty, Friedman, and Gal [3], including the then available precise measurements of W and Pb atoms and employing phenomenological density-dependent fits, has led to a  $\Sigma$ -nucleus potential with a strongly repulsive core (of height  $\sim 95 \text{ MeV}$ ) and a shallow attractive tail outside the nucleus. However, because of the poor penetration of the  $\Sigma^-$  hyperon into the nucleus, such fitted potentials are not well defined by the  $\Sigma^-$ -atom data in the nuclear interior. The inclusive ( $\pi^-$ ,  $K^+$ ) spectra on medium-to-heavy nuclear targets measured at KEK [4,5] give more direct evidence for a strongly repulsive  $\Sigma$ -nucleus potential. In the framework of the distorted-wave impulse approximation, a best fit of the measured ( $\pi^-$ ,  $K^+$ ) inclusive spectra on Si, Ni, In, and Bi targets is obtained with a  $\Sigma$ -nucleus repulsion of about  $90 \text{ MeV}$  [5]. In addition, a nonzero value of the imaginary  $\Sigma$ -nucleus potential (with a best fit value of about  $-40 \text{ MeV}$  [5]) is also required in order to reproduce the observed spectra of the double differential cross section  $d^2\sigma/d\Omega dE$ . Very recently, Kohno *et al.* [6] have calculated the ( $\pi^-$ ,  $K^+$ ) inclusive spectra on Si within a semiclassical distorted wave model, and they found that the KEK data can also be well reproduced with a complex  $\Sigma$ -nucleus potential of strength  $(30 - 20i) \text{ MeV}$ . The different result from Ref. [5] may be due to avoiding the factorization approximation by using an average cross section [6]. For an up-to-date and comprehensive overview of hypernuclear physics, see Ref. [7].

In the standard one-boson exchange models for hyperon-nucleon interaction, there are appreciable uncertainties in

various meson-baryon coupling constants, although SU(3) relations are imposed. Most of these models give an attractive (real)  $\Sigma$ -nucleus potential [8–10], but the Nijmegen model F [11] leads to repulsion, estimated to be about  $(4-8i) \text{ MeV}$  in nuclear matter [12]. A nonrelativistic SU(6) quark model for the unifying description of octet baryon-baryon interactions has been developed by the Kyoto-Niigata group [13].  $G$ -matrix calculations in lowest order Brueckner theory [14] with this hyperon-nucleon interaction showed that the real part of the  $\Sigma$  nuclear mean field is repulsive of the order of  $20 \text{ MeV}$  due to a strong repulsion in the total  $\Sigma N$ -isospin  $3/2$  channel which originates from Pauli blocking effects at the quark level. The same calculation [14] has found an imaginary part of the  $\Sigma$  single-particle potential in nuclear matter of  $-20 \text{ MeV}$ , comparable to the value  $-16 \text{ MeV}$  extracted in the earlier analysis of the  $\Sigma^-$ -atom data [1]. The basic physical mechanism behind this sizeable (negative) imaginary part is, of course, the strong conversion process  $\Sigma N \rightarrow \Lambda N$  in nuclear matter.

More recently, chiral effective field theory approaches have opened new perspectives for dealing with binding and saturation of nuclear matter as well as single-particle properties of nucleons [15] and  $\Lambda$  hyperons [16] in the nuclear medium. A key element in these approaches is the separation of long- and short-distance dynamics and an ordering scheme in powers of small momenta. At nuclear matter saturation density  $\rho_0 = 0.16 \text{ fm}^{-3}$ , the Fermi momentum  $k_{f0}$  and the pion mass  $m_{\pi}$  are comparable scales ( $k_{f0} \simeq 2m_{\pi}$ ), and therefore pions must be included as explicit degrees of freedom in the description of the nuclear many-body dynamics. In this work, we extend such a field-theoretical approach to the complex single-particle potential of a  $\Sigma$  hyperon in isospin-symmetric nuclear matter.

Our calculation is based on the leading order chiral meson-baryon Lagrangian in flavor SU(3) [17],

$$\mathcal{L}_{\phi B} = \frac{D}{2f_{\pi}} \text{tr}(\bar{B} \vec{\sigma} \cdot \{\vec{\nabla}\phi, B\}) + \frac{F}{2f_{\pi}} \text{tr}(\bar{B} \vec{\sigma} \cdot [\vec{\nabla}\phi, B]) + \dots, \quad (1)$$

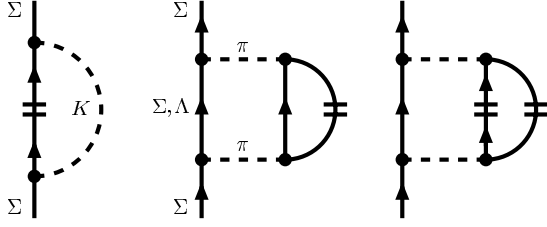


FIG. 1. One-kaon exchange Fock diagram and iterated one-pion exchange Hartree diagrams with  $\Sigma$  or  $\Lambda$  hyperons in the intermediate state. The horizontal double line symbolizes the filled Fermi sea of nucleons, i.e., the medium insertion  $-\theta(k_f - |\vec{p}|)$  in the in-medium nucleon propagator [15]. Effectively, the medium insertion sums up hole propagation and the absence of particle propagation below the Fermi surface  $|\vec{p}| < k_f$ .

where the traceless hermitian  $3 \times 3$  matrices  $B$  and  $\phi$  collect the octet baryon fields ( $N, \Lambda, \Sigma, \Xi$ ) and the pseudoscalar Goldstone bosons fields ( $\pi, K, \bar{K}, \eta$ ), respectively. The parameter  $f_\pi = 92.4$  MeV is the weak pion decay constant, and  $D$  and  $F$  denote the SU(3) axial-vector coupling constants of the octet baryons. We choose as their values  $D = 0.84$  and  $F = 0.46$ . This leads to a  $KN\Sigma$  coupling constant of  $g_{KN\Sigma} = (D - F)(M_N + M_\Sigma)/(2f_\pi) = 4.4$ , a  $\pi\Lambda\Sigma$  coupling constant of  $g_{\pi\Lambda\Sigma} = D(M_\Lambda + M_\Sigma)/(\sqrt{3}f_\pi) = 12.1$ , and a  $\pi\Sigma\Sigma$  coupling constant of  $g_{\pi\Sigma\Sigma} = 2FM_\Sigma/f_\pi = 11.9$ , consistent with the empirical values summarized in Tables 6.3 and 6.4 of Ref. [18]. The  $\pi\Lambda\Sigma$  coupling constant used in the present work is also consistent with the value  $g_{\pi\Lambda\Sigma} = 12.9 \pm 0.9$  extracted recently from hyperonic atom data in Ref. [19]. Furthermore, the pion-nucleon coupling constant has the value  $g_{\pi N} = g_A M_N/f_\pi = 13.2$  [20], with  $g_A = D + F = 1.3$ . The ellipsis in Eq. (1) stands for the chiral-invariant interaction terms with two or more Goldstone boson fields, which do not come into play in the present calculation.

Consider the density-dependent complex self-energy  $U_\Sigma(k_f) + iW_\Sigma(k_f)$  of a zero-momentum  $\Sigma$  hyperon ( $\vec{p}_\Sigma = \vec{0}$ ) placed as a test particle into isospin-symmetric nuclear matter. The value  $U_\Sigma(k_{f0}) + iW_\Sigma(k_{f0})$  at nuclear matter saturation density  $\rho_0 = 0.16$  fm $^{-3}$  fixes the strength of the  $\Sigma$ -nucleus optical potential. We calculate the long-range contributions to the  $\Sigma$  nuclear mean field  $U_\Sigma(k_f) + iW_\Sigma(k_f)$  generated by the exchange of light Goldstone bosons between the  $\Sigma$  hyperon and the nucleons in the filled Fermi sea. The only nonvanishing one-meson exchange contribution comes from the kaon-exchange Fock diagram in Fig. 1, from which we obtain the (small and) repulsive contribution to the real part of the  $\Sigma$  nuclear mean field,

$$U_\Sigma(k_f)^{(K)} = \frac{(D - F)^2}{(2\pi f_\pi)^2} \left\{ \frac{k_f^3}{3} - m_K^2 k_f + m_K^3 \arctan \frac{k_f}{m_K} \right\}, \quad (2)$$

with  $m_K = 496$  MeV the average kaon mass. At densities at and below nuclear matter saturation density  $\rho \leq 0.16$  fm $^{-3}$  (corresponding to Fermi momenta  $k_f \leq 263$  MeV), the kaon exchange can already be regarded as short range. The ratio  $k_f/m_K \leq 0.53$  is small, and the expression in curly brackets

in Eq. (2) is dominated by its leading term  $k_f^3/5m_K^2$  in the  $k_f$  expansion.

The truly long-range interaction between the  $\Sigma$  hyperon and the nucleons arises therefore from two-pion exchange. The corresponding two-loop diagrams with a  $\Sigma$  or a  $\Lambda$  hyperon in the intermediate state are shown in Fig. 1. Their relative isospin factor (for the  $\Sigma$ - and  $\Lambda$ -intermediate state) is  $6(F/D)^2 \simeq 1.8$ . We find from the second diagram in Fig. 1, with one medium insertion [15] and a  $\Sigma$  hyperon in the intermediate state, the following long-range contribution to the real part of the  $\Sigma$  nuclear mean field,<sup>1</sup>

$$U_\Sigma(k_f)^{(2\pi\Sigma)} = \frac{F^2 g_A^2 M_B m_\pi^2}{8\pi^3 f_\pi^4} \times \left[ -3m_\pi k_f + (2k_f^2 + 3m_\pi^2) \arctan \frac{k_f}{m_\pi} \right], \quad (3)$$

with  $m_\pi = 138$  MeV the average pion mass. The mean baryon mass  $M_B = (2M_N + M_\Lambda + M_\Sigma)/4 = 1047$  MeV serves the purpose of averaging out small differences in the kinetic energies of the various baryons involved. Note the large scale enhancement factor  $M_B$  in Eq. (3) which stems from the energy denominator of the  $2\pi$ -exchange diagram. Because of this characteristic property, the notion of iterated (second order) one-pion exchange is actually more appropriate (see also Sec. 4 in Ref. [21] for the analogous classification of the  $2\pi$ -exchange  $NN$  interaction). The third diagram in Fig. 1 with two medium insertions represents a Pauli blocking correction. With an intermediate  $\Sigma$  hyperon, the contribution to the real part of the  $\Sigma$  nuclear mean field can be expressed as

$$U_\Sigma(k_f)_{\text{Pauli}}^{(2\pi\Sigma)} = \frac{F^2 g_A^2 M_B}{(2\pi f_\pi)^4} \left\{ 2k_f^4 - m_\pi^4 \int_0^u dx \times \int_{-1}^1 \frac{dz}{z} \left[ \frac{1}{S} + 2 \ln S \right] \right\}, \quad (4)$$

with the auxiliary function  $S = 1 + u - x + 2xz^2 + 2z\sqrt{x(u - x + xz^2)}$  and the abbreviation  $u = k_f^2/m_\pi^2$ . The symbol  $\int_{-1}^1 dz$  in Eq. (4) denotes a principal value integral. We also note that the total imaginary part  $W_\Sigma(k_f)^{(2\pi\Sigma)} + W_\Sigma(k_f)_{\text{Pauli}}^{(2\pi\Sigma)}$  vanishes identically.

Next, we come to the iterated one-pion exchange diagrams with an intermediate  $\Lambda$  hyperon. The small  $\Sigma\Lambda$ -mass splitting  $M_\Sigma - M_\Lambda = 77.5$  MeV, which comes into play here, is comparable in magnitude to the typical kinetic energies of the nucleons. Therefore, it has to be counted accordingly in the energy denominator. By the relation  $M_\Sigma - M_\Lambda = \Delta^2/M_B$ , we introduce another small mass scale  $\Delta$ , whose magnitude  $\Delta \simeq 285$  MeV is close to the Fermi momentum  $k_{f0} \simeq 263$  MeV at nuclear matter saturation density. Putting all the pieces together, we find from the second

<sup>1</sup>We have used dimensional regularization (where a linear divergence  $\int_0^\infty dl$  is set to zero) to evaluate the loop integral. In cutoff regularization, one would get in addition a term linear in the cutoff and the density  $\rho$ . Since such a term is indistinguishable from the effect of a zero-range contact interaction, it does not belong to the genuine long-range contributions.

diagram in Fig. 1 with an intermediate  $\Lambda$  hyperon the following long-range contribution to the complex  $\Sigma$  nuclear mean field

$$U_{\Sigma}(k_f)^{(2\pi\Lambda)} + i W_{\Sigma}(k_f)^{(2\pi\Lambda)} = \frac{D^2 g_A^2 M_B m_{\pi}^4}{48\pi^3 f_{\pi}^4} \Psi\left(\frac{k_f^2}{m_{\pi}^2}, \frac{\Delta^2}{m_{\pi}^2}\right), \quad (5)$$

where the complex function

$$\begin{aligned} \Psi(u, \delta) = & -(\delta + 3)\sqrt{u} - \frac{i}{4}(u + 2\delta + 6)\sqrt{u(4\delta + u)} \\ & + (2u + \delta^2 + 4\delta + 3) \left\{ \arctan \frac{\sqrt{u}}{1 + \delta} \right. \\ & \left. + i \ln \frac{2 + 2\delta + u + \sqrt{u(4\delta + u)}}{2[(1 + \delta)^2 + u]^{1/2}} \right\} \end{aligned} \quad (6)$$

emerges from the combined loop and Fermi sphere integration with the abbreviation  $\delta = \Delta^2/m_{\pi}^2$ . The corresponding Pauli blocking correction to the real part of the  $\Sigma$  nuclear mean field can be expressed as a numerically easily manageable double integral of the form

$$\begin{aligned} U_{\Sigma}(k_f)_{\text{Pauli}}^{(2\pi\Lambda)} = & \frac{D^2 g_A^2 M_B m_{\pi}^4}{6(2\pi f_{\pi})^4} \int_0^u dx \int_0^u dy \frac{1}{(2\delta + 1 + x - y)^2} \\ & \times \left[ \frac{4(y - x - 2\delta - 1)\sqrt{xy}}{(1 + x + y)^2 - 4xy} \right. \\ & + (2x - 2y + 4\delta + 1) \ln \frac{1 + x + y + 2\sqrt{xy}}{1 + x + y - 2\sqrt{xy}} \\ & \left. + (2\delta + x - y)^2 \ln \frac{|\delta - y - \sqrt{xy}|}{|\delta - y + \sqrt{xy}|} \right]. \end{aligned} \quad (7)$$

In the case of the imaginary part of the  $\Sigma$  nuclear mean field, the Pauli blocking correction can even be written in closed analytical form:

$$\begin{aligned} W_{\Sigma}(k_f)_{\text{Pauli}}^{(2\pi\Lambda)} = & \frac{D^2 g_A^2 M_B m_{\pi}^4}{96\pi^3 f_{\pi}^4} \theta(\sqrt{2}k_f - \Delta) \\ & \times \left[ \frac{u^2}{4} + \frac{3}{2}(u - \delta^2) + (u - 3)\delta \right. \\ & + \frac{1}{4}(u + 2\delta + 6)\sqrt{u(4\delta + u)} - (2u + \delta^2) \\ & \times \ln \frac{2 + 2\delta + u + \sqrt{u(4\delta + u)}}{2 + 2u^{-1}\delta^2} - (3 + 4\delta) \\ & \left. \times \ln \frac{2 + 2\delta + u + \sqrt{u(4\delta + u)}}{2 + 4\delta} \right]. \end{aligned} \quad (8)$$

It is interesting to observe that there is a threshold condition  $k_f > \Delta/\sqrt{2}$  for Pauli blocking to become active in the imaginary part of the  $\Sigma$  nuclear mean field. This threshold corresponds to the subnuclear density  $\rho_{\text{th}} = 0.072 \text{ fm}^{-3} = 0.45 \rho_0$ . Furthermore, as a simple check, one verifies that the total imaginary  $\Sigma$  nuclear mean field  $W_{\Sigma}(k_f)^{(2\pi\Lambda)} + W_{\Sigma}(k_f)_{\text{Pauli}}^{(2\pi\Lambda)}$  vanishes identically in the limit of  $\Sigma\Lambda$ -mass degeneracy, i.e.,  $\delta = 0$ . We have also evaluated the contributions to  $U_{\Sigma}(k_f)$

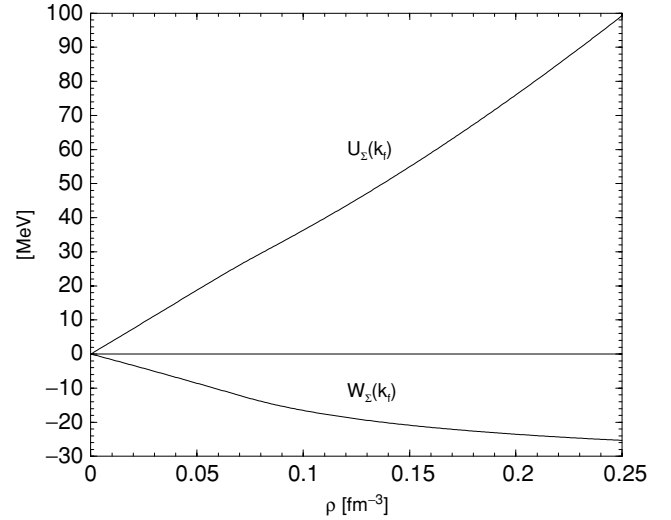


FIG. 2. The complex mean field  $U_{\Sigma}(k_f) + iW_{\Sigma}(k_f)$  of a zero-momentum  $\Sigma$  hyperon in isospin-symmetric nuclear matter versus the nucleon density  $\rho = 2k_f^3/3\pi^2$ . The imaginary part  $W_{\Sigma}(k_f)$  (lower solid line) originates from the conversion process  $\Sigma N \rightarrow \Lambda N$  induced by one-pion exchange. The real part  $U_{\Sigma}(k_f)$  (upper solid line) includes only genuine long-range contributions.

from irreducible two-pion exchange (which do not carry the large scale enhancement factor  $M_B$ ) and found that they sum up to zero in isospin-symmetric nuclear matter. For comparison, the same exact cancellation is at work in the isoscalar central channel of the  $2\pi$ -exchange  $NN$  potential (see Sec. 4.2 in Ref. [21]). As an aside, we note that the Pauli blocking corrections Eqs. (4, 7, 8) could also be interpreted as the effects of the  $2\pi$ -exchange  $\Sigma NN$  three-body interaction [22]. This equivalence becomes immediately clear by opening the two nucleon lines (with horizontal double lines) of the last diagram in Fig. 1.

Summing up all calculated terms, we show in Fig. 2 the resulting complex  $\Sigma$  nuclear mean field  $U_{\Sigma}(k_f) + iW_{\Sigma}(k_f)$  as a function of the nucleon density  $\rho = 2k_f^3/3\pi^2$ . The lower curve for the imaginary part  $W_{\Sigma}(k_f)$  displays clearly the onset of the Pauli blocking effects at the threshold density  $\rho_{\text{th}} = 0.072 \text{ fm}^{-3}$ . It is very astonishing that the total real  $\Sigma$  nuclear mean field  $U_{\Sigma}(k_f)$  follows to a good approximation a straight line, whereas individual components possess a much more nonlinear dependence on the density  $\rho$ , driven by the relevant dimensionless variable  $\sqrt{u} = k_f/m_{\pi}$ . At normal nuclear matter density  $\rho_0 = 0.16 \text{ fm}^{-3}$  (corresponding to a Fermi momentum of  $k_{f0} = 263 \text{ MeV}$ ), one finds for the real and imaginary part, respectively  $U_{\Sigma}(k_{f0}) = [0.4 + (40.9 + 16.1) + (8.2 - 6.6)] \text{ MeV} = 59 \text{ MeV}$  and  $W_{\Sigma}(k_{f0}) = (-29.0 + 7.5) \text{ MeV} = -21.5 \text{ MeV}$ , where the individual entries correspond to the respective terms written in Eqs. (2)–(8), in that order. As could be expected from the small  $KN\Sigma$  coupling constant  $g_{KN\Sigma} = 4.4$ , the kaon-exchange contribution is completely negligible. The genuine long-range terms from iterated one-pion exchange with the intermediate  $\Sigma$  and  $\Lambda$  hyperons written in Eqs. (3),(5) build up a sizeable repulsion of 49 MeV which is furthermore enhanced (by about 20%) by the Pauli blocking corrections of Eqs. (4),(7). Note

that one is dealing here with six-dimensional principal value integrals whose signs are not a priori fixed. The imaginary single-particle potential of  $W_{\Sigma}(k_{f0}) = -21.5$  MeV comes out surprisingly close to the value  $-20$  MeV obtained in the SU(6) quark model calculation of Ref. [14] or the value  $-16$  MeV extracted from  $\Sigma^-$ -atom data [1]. Of course, in order to account for the uncertainties in the axial-vector coupling constants  $D$  and  $F$ , and the choice of a mean baryon mass  $M_B$ , one should add to the curves in Fig. 2 an error band of at least  $\pm 20\%$ . Moreover, there are recoil corrections to the leading order results given in Eqs. (2)–(8). Since these recoil corrections scale (at least) as  $1/M_B$  with the baryon mass  $M_B$ , they are expected to be suppressed by the small relative factor  $(k_f/M_B)^2 \leq 0.07$  (for moderate densities  $\rho \leq 0.2$  fm $^{-3}$ ). If one continues the curves in Fig. 2 to even higher densities  $\rho \leq 0.5$  fm $^{-3}$ , one finds a stronger than linear rise of the real part  $U_{\Sigma}(k_f)$ , and an approximate saturation of the imaginary part  $U_{\Sigma}(k_f)$  at a value of about  $-30$  MeV. However, this behavior should not be taken too seriously, since for Fermi momenta  $k_f > 350$  MeV, one presumably exceeds the limits of validity of the present calculation based on in-medium chiral perturbation theory (see also the discussion in Ref. [15]).

Altogether, it seems that the leading long-range two-pion exchange dynamics evaluated in the present field-theoretical approach is able to reproduce qualitatively the single-particle properties of  $\Sigma$  hyperons in the nuclear medium in agreement with existing phenomenology and more sophisticated model calculations. This raises a question about the role of the short-range  $\Sigma N$  interaction (and additional short-range correlations). QCD sum rule calculations of  $\Sigma$  hyperons in nuclear matter [23] indicate that the individually large Lorentz scalar and vector mean fields (typically of strength  $\mp 0.2M_{\Sigma}$ ) cancel each other to a large extent. In the case of the Lorentz scalar mean field, the QCD sum rule results are subject to large uncertainties due to unknown contributions from four-quark condensates. Conversely, at least some of these contributions are accounted for by our explicit treatment of the long-range two-pion exchange processes. A combined QCD sum rule analysis of nucleons,  $\Lambda$  hyperons, and  $\Sigma$  hyperons in nuclear

matter together with input from in-medium chiral perturbation theory and phenomenology should help to better constrain the short-distance baryon-nucleon dynamics (whose details are, however, not resolved at the scale of the nuclear Fermi momentum  $k_{f0}$ ).

In summary, we have calculated in this work the density-dependent complex mean field  $U_{\Sigma}(k_f) + iW_{\Sigma}(k_f)$  of a  $\Sigma$  hyperon in isospin-symmetric nuclear matter in the two-loop approximation of in-medium chiral perturbation theory. The leading long-range  $\Sigma N$  interaction arises from iterated (second order) one-pion exchange with a  $\Sigma$  or  $\Lambda$  hyperon in the intermediate state. These second order pion-exchange contributions do not correspond to any mean field Hartree approximation as evidenced by their intrinsic nonlinear density dependence. To the order in the small momentum expansion we are working with here, the long-range correlations between the  $\Sigma$  hyperon and the nucleons are fully taken into account. We find from the strong  $\Sigma N \rightarrow \Lambda N$  conversion process at nuclear matter saturation density  $\rho_0 = 0.16$  fm $^{-3}$  an imaginary single-particle potential of  $W_{\Sigma}(k_{f0}) = -21.5$  MeV. The genuine long-range contributions from iterated pion-exchange sum up to a moderately repulsive real single-particle potential of  $U_{\Sigma}(k_{f0}) = 59$  MeV. Taking into account the uncertainties of the involved coupling constants, such values are already compatible with the  $\Sigma$ -nucleus optical potential needed to describe the inclusive ( $\pi^-$ ,  $K^+$ ) spectra related to  $\Sigma^-$  formation in heavy nuclei. Our results suggest that the net effect of the short-range  $\Sigma N$  interaction on the  $\Sigma$  nuclear mean field could be small. A combined QCD sum rule analysis of nucleons,  $\Lambda$  hyperons, and  $\Sigma$  hyperons in nuclear matter can help to clarify the latter point. Furthermore, the present calculation can easily be extended to nonzero  $\Sigma$ -momentum  $p$ , and from the corresponding momentum and density-dependent mean field  $U_{\Sigma}(p, k_f) + iW_{\Sigma}(p, k_f)$ , one can extract, for example, an effective  $\Sigma$  mass [22,24]. Work along these lines is in progress.

I thank A. Gal, G. Lalazissis, and W. Weise for informative discussions.

- 
- [1] C. B. Dover, D. J. Millener, and A. Gal, Phys. Rep. **184**, 1 (1989), and references therein.
- [2] R. E. Chrien and C. B. Dover, Annu. Rev. Nucl. Part. Sci. **39**, 113 (1989), and references therein.
- [3] C. J. Batty, E. Friedman, and A. Gal, Phys. Rep. **287**, 385 (1997), and references therein.
- [4] H. Noumi *et al.*, Phys. Rev. Lett. **89**, 072301 (2002); **90**, 049902(E) (2003).
- [5] P. K. Saha *et al.*, Phys. Rev. C **70**, 044613 (2004).
- [6] M. Kohno *et al.*, Prog. Theor. Phys. **112**, 895 (2004).
- [7] A. Gal, Prog. Theor. Phys. Suppl. **156**, 1 (2004).
- [8] R. Brockmann and E. Oset, Phys. Lett. **B118**, 33 (1982).
- [9] H. J. Schulze, M. Baldo, U. Lombardo, J. Cugnon, and A. Lejeune, Phys. Rev. C **57**, 704 (1998).
- [10] Y. Yamamoto, S. Nishizaki, and T. Takatsuka, Prog. Theor. Phys. **103**, 981 (2000), and references therein.
- [11] Th. A. Rijken, V. G. J. Stoks, and Y. Yamamoto, Phys. Rev. C **59**, 21 (1999), and references therein.
- [12] T. Yamada and Y. Yamamoto, Prog. Theor. Phys. Suppl. **117**, 241 (1994).
- [13] Y. Fujiwara, M. Kohno, C. Nakamoto, and Y. Suzuki, Phys. Rev. C **64**, 054001 (2001), and references therein.
- [14] M. Kohno *et al.*, Nucl. Phys. **A674**, 229 (2000).
- [15] N. Kaiser, S. Fritsch, and W. Weise, Nucl. Phys. **A697**, 255 (2002); **A700**, 343 (2002); **A750**, 259 (2005).
- [16] N. Kaiser and W. Weise, Phys. Rev. C **71**, 015203 (2005).
- [17] V. Bernard, N. Kaiser, and Ulf-G. Meißner, Int. J. Mod. Phys. E **4**, 193 (1995).
- [18] O. Dumbrajs *et al.*, Nucl. Phys. **B216**, 277 (1983).
- [19] B. Loiseau and S. Wycech, Phys. Rev. C **63**, 034003 (2001).
- [20] M. M. Pavan *et al.*, Phys. Scr. **T87**, 65 (2000).
- [21] N. Kaiser, R. Brockmann, and W. Weise, Nucl. Phys. **A625**, 758 (1997).
- [22] Q. N. Usmani and A. R. Bodmer, Phys. Rev. C **60**, 055215 (1999).
- [23] X. Jin and M. Nielsen, Phys. Rev. C **51**, 347 (1995), and references therein.
- [24] D. J. Millener, Nucl. Phys. **A691**, 93c (2001).